

Fractional Crystallization of Hanford Single-Shell Tank Wastes A Modeling Approach

D.J. Geniesse, E.A. Nelson

AREVA NC Inc.

2425 Stevens Center Place, Second Floor
Richland, WA 99352
USA

D.W. Hamilton

CH2M HILL Hanford Group, Inc.
P.O. Box 1500, Richland, WA 99352-1505
USA

ABSTRACT

An advanced thermodynamic modeling technique has been utilized to establish the feasibility of using fractional crystallization to pretreat Hanford Site tank waste. The Hanford site has 149 underground single-shell tanks (SST) storing mostly soluble, multi-salt, mixed radioactive wastes resulting from Cold War era weapons material production. The solubility of a particular species depends on its concentration, temperature of the solution and the presence of other ionic species in the solution. By establishing the proper conditions, selected pure salts can be crystallized and separated from the radioactive liquid phase. Since the Hanford wastes contain many different ions competing for solubility (dominant ones are Na^{+1} , NO_3^{-1} , CO_3^{-2} , and SO_4^{-2}) a thermodynamic modeling tool was used to determine conditions for maximum salt removal. The modeling program is commercially available software operating on a database compiled from years of chemical analyses of the SST contents. The model was used extensively to develop and guide laboratory experiments demonstrating the fractional crystallization process which began with crystallizing simple salt solutions, progressed to a well characterized non-radioactive simulant, and culminated in actual radioactive waste testing.

INTRODUCTION

The Hanford site has 149 underground SST storing mostly soluble, multi-salt, mixed wastes resulting from Cold War era weapons material production. These wastes must be retrieved and the salts immobilized before the tanks can be closed to comply with an overall site closure consent order entered into by the U.S. Department of Energy, the Environmental Protection Agency, and Washington State. Water will be used to retrieve the wastes and the resulting solution will be pumped to the proposed treatment process where a high curie (primarily Cs-137) waste fraction will be separated from the other waste constituents. The separated waste streams will then be vitrified to allow for safe storage as an immobilized high level waste, or low level waste, borosilicate glass.

Fractional crystallization, a common unit operation for production of industrial chemicals and pharmaceuticals, was proposed as the method to separate the salt wastes; it works by evaporating excess water until the solubilities of various species in the solution are exceeded (the solubility

of a particular species depends on its concentration, temperature of the solution, and the presence of other ionic species in the solution). By establishing the proper conditions for the Hanford waste simulant and actual tank waste, selected pure salts can be crystallized and separated from the radioactive liquid phase. To establish the proper conditions to guide laboratory experiments a thermodynamic model was used. The model uses thermodynamic properties to determine aqueous speciation equilibrium reactions.

MODELING APPROACH

In multi-component Hanford waste, the solubility of components cannot be predicted from solubility diagrams or by hand calculation techniques because of the complexity of the chemistry. Solubility of components is a function of the water content, initial concentrations of the salts, free hydroxide, temperature, and ionic strength. To predict the solubility of components, the yield during crystallization, and the extent of decontamination, computational thermodynamic models are used.

Environmental Simulation Program (ESP) software, leased from OLI Systems (Morris Plains, NJ), has been enhanced to simulate high ionic strength aqueous systems, such as Hanford waste. Recently, improvements were made in the sodium carbonate, sulfate, fluoride, nitrate, and nitrite databanks [1] to accurately predict sodium salt solubilities and physical properties of Hanford waste. The ESP model was used for the development of the solubility phase diagrams and evaporation survey graphs presented in this report. Mixed Solvent Electrolyte (MSE) software has recently been developed by OLI systems to model high ionic strength solutions such as crystallization liquors. The software is more stable than ESP; however at this time it is not as accurate as the ESP software using the WTPBASE databank.

Process thermodynamic modeling has been performed on Hanford waste simulant chemistries to develop the preliminary fractional crystallization (FC) process flowsheets and determine the maximum theoretical yield of sodium salts in fractional crystallization processes.

Soluble alumina salts, e.g. sodium aluminate (NaAlO_2), resulting from spent nuclear fuel processing are contained in the tank wastes. To maintain the alumina in solution, substantial amounts of sodium salts (NaOH , Na_2CO_3 , etc.) are needed and if these salts are removed by the FC process to obtain current required sodium yields (> 50% sodium removal), an alumina gel can form in tank wastes with high soluble alumina content. One way to obtain high sodium yield is to remove the alumina through Gibbsite ($\text{Al}(\text{OH})_3$) crystallization; however, alumina removal is not currently included in the scope of the FC process

The utility of modeling the waste components can be demonstrated by the following examples:

Sodium Sulfate-Sodium Carbonate Solubility

Depending on relative abundance, sodium sulfate double salts may crystallize first upon evaporation of waste liquor. Dominant sulfate salts are the sodium sulfate-carbonate double salt burkeite ($\text{Na}_6(\text{SO}_4)_2\text{CO}_3$) or the sodium sulfate-fluoride double salt shairerite (Na_3FSO_4).

The phase diagram, developed using the ESP model, for the $\text{H}_2\text{O}-\text{Na}_2\text{SO}_4-\text{Na}_2\text{CO}_3$ ternary system is shown in Figure 1.

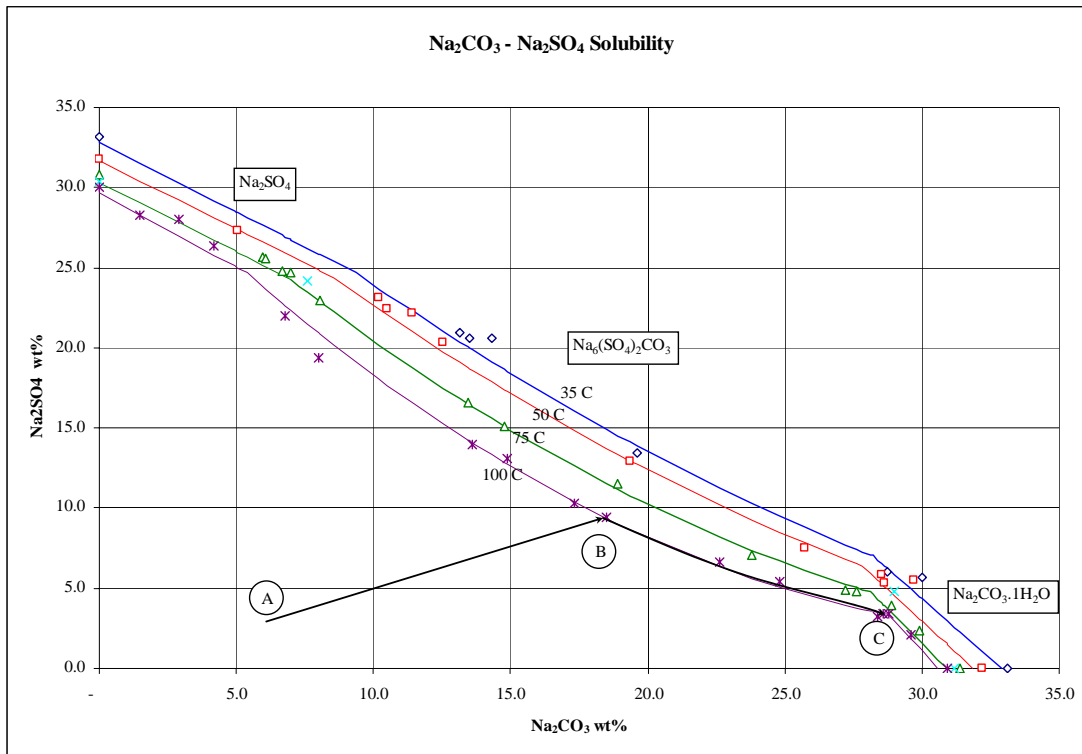


Fig. 1. $\text{NaSO}_4\text{-NaCO}_3$ Solubility (U.S. Patent 6,787,120).

Operating line A-B depicts a solution with an initial concentration of 3 wt % Na_2SO_4 and 6 wt% Na_2CO_3 evaporated to saturation at 100°C. Burkeite saturation is reached after 75 g H_2O are evaporated, at a concentration of 9 wt% Na_2SO_4 and 18 wt% Na_2CO_3 and at an ionic strength of 9 M sodium. Further evaporation crystallizes $\text{Na}_6(\text{SO}_4)_2\text{CO}_3$ [2], depleting the solution of sodium sulfate and carbonate in a 2:1 mole ratio and follows the saturation curve from B to C. At point C, 88 g of water have evaporated and 3.3 g $\text{Na}_6(\text{SO}_4)_2\text{CO}_3$ have crystallized from solution at a concentration of 3.3 wt% Na_2SO_4 and 29 wt% Na_2CO_3 and an ionic strength of 12 M Na.

Sodium carbonate monohydrate ($\text{Na}_2\text{CO}_3 \cdot 1\text{H}_2\text{O}$) reaches saturation at point C and co-crystallizes with burkeite upon further evaporation. In a binary $\text{H}_2\text{O}\text{-Na}_2\text{CO}_3$ system, the monohydrate crystal typically forms between 35°C and 106°C; sodium carbonate decahydrate ($\text{Na}_2\text{CO}_3 \cdot 10\text{H}_2\text{O}$) forms below 35°C. However, in multi-component Hanford waste, the stability range of sodium carbonate monohydrate is extended below 35°C due to low water activity (concentration).

As shown in Figure 1 above, further evaporation at point C co-crystallizes $\text{Na}_6(\text{SO}_4)_2\text{CO}_3$ and $\text{Na}_2\text{CO}_3 \cdot 1\text{H}_2\text{O}$ in equimolar proportions, so the solution is depleted in sodium sulfate and sodium carbonate in the same proportions. At this point, ionic strength remains constant at 12 M. At the invariant point, the relative concentrations of sodium carbonate and sulfate in solution remain the same while the two salts co-crystallize.

At the invariant point, additional sodium carbonate-sulfate double salts may form such as “high carb” burkeite $\text{Na}_6\text{SO}_4(\text{CO}_3)_2$. [3] The additional salts deplete the aqueous phase of sodium sulfate and carbonate upon further evaporation.

Sodium Nitrate-Sodium Nitrite Solubility

The behavior of sodium nitrite and nitrate vary depending on other ions present and evaporation temperatures.

Depending on relative abundance, sodium nitrate and/or sodium nitrite may crystallize upon further evaporation. In other cases, sodium nitrate and/or nitrite will co-crystallize with burkeite and/or sodium carbonate monohydrate. In some cases, sodium nitrate and nitrite will not reach saturation until all of the sodium sulfate and carbonate are depleted from the aqueous phase. In other cases, sodium nitrate or sodium nitrite will reach saturation and crystallize before the sodium sulfate or carbonate reach saturation.

A phase diagram of sodium nitrate and nitrite is shown in Figure 2. Sodium nitrate and sodium nitrite exhibit temperature-dependant and complementary solubility. The solubility of each species increases with temperature.

The two species form a “eutectic” in which the total sodium solubility is increased when both species are present. The solubility of a two-salt system increases with further evaporation up to the $\text{NaNO}_3\text{-NaNO}_2$ invariant – the point where the two salts co-crystallize. Thus, a ternary solution containing $\text{H}_2\text{O}\text{-NaNO}_3\text{-NaNO}_2$ has greater solubility than binary solutions of $\text{H}_2\text{O}\text{-NaNO}_3$ or $\text{H}_2\text{O}\text{-NaNO}_2$.

In binary solutions at 52°C, the solubility of NaNO_3 is 118 g/100 g H_2O ; the solubility of NaNO_2 is 109 g/100 g H_2O . In a ternary $\text{H}_2\text{O}\text{-NaNO}_3\text{-NaNO}_2$ system, the total solubility increases to 182 g $\text{NaNO}_3 + \text{NaNO}_2$ /100 g H_2O at the $\text{NaNO}_3\text{-NaNO}_2$ invariant point.

The increase in solubility upon evaporation is shown by the operating lines A-B and B-C. An initial solution of 100 g H_2O , 40 g NaNO_3 , and 10 g NaNO_2 (Point A) is evaporated to NaNO_3 saturation (Point B). The solution is further evaporated to NaNO_2 saturation (Point C). At a total of 90 g of H_2O evaporated, the net yield of NaNO_3 is 33 g or 62.6% of the total sodium. During crystallization, ionic strength increases from 15 M to 21 M Na.

Because the solubility is temperature dependent, the crystallization yield may be increased by reducing temperature. In the above example, if the evaporation occurred at 40°C, the sodium yield would be 68.3% at 90 g of water evaporated. Ionic strength at this point is 19.2 M Na.

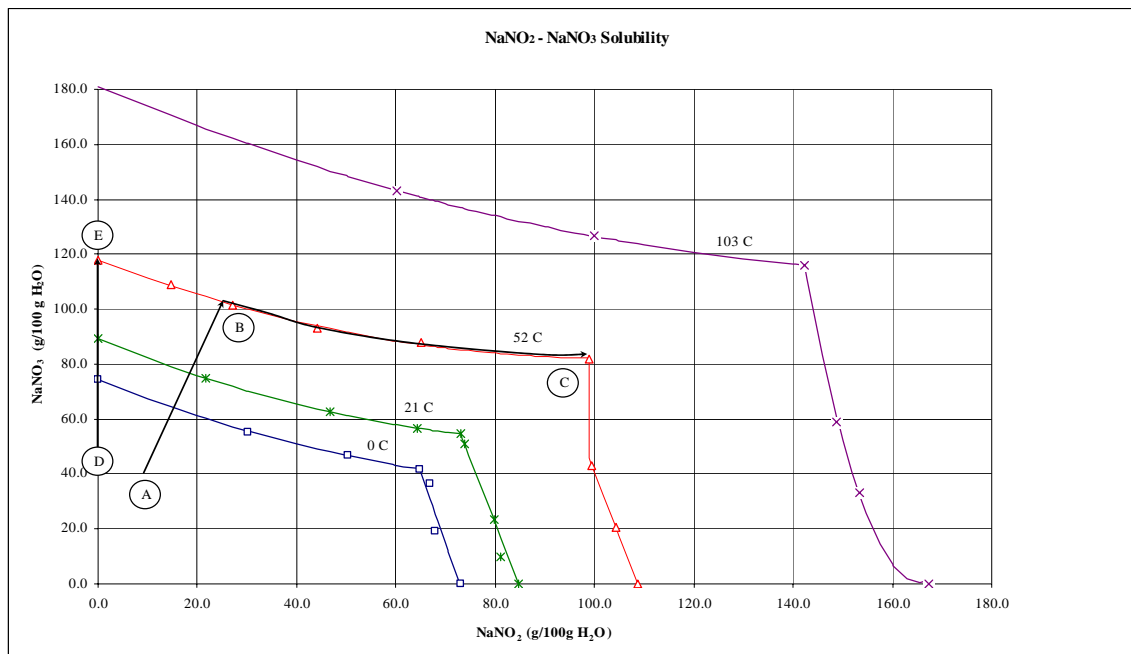


Fig. 2. Phase diagram of sodium nitrate and nitrite.

Thus, reducing temperature can increase the yields of sodium nitrate and nitrite in a batch evaporation process at constant ionic strength.

Alumina Solubility

A diagram of alumina solubility versus free hydroxide is shown in Figure 3. This diagram is valid for alkaline solutions only, where $\text{Al}(\text{OH})_4^-$ is the dominant aqueous specie.

The solid lines (ESP) are isotherms in a ternary $\text{Al}(\text{OH})_3$ - NaOH - H_2O system. [4] The dashed lines (ESP MIX) are in a multi-component $\text{Al}(\text{OH})_3$ - NaOH - H_2O system saturated with Na_2CO_3 , Na_2SO_4 , NaNO_2 , and NaNO_3 . Experimental points (APPS) on the graph are from the J.A. Apps report. [5] Thermodynamic state properties (G_f , H_f , S_f) of gibbsite $\text{Al}(\text{OH})_3$, used in the calculation of alumina solubility, were developed in the Apps study.

As shown in the diagram, alumina solubility is a complex function of temperature, free hydroxide, and ionic strength. Increasing ionic strength by addition of additional sodium species increases gibbsite solubility but decreases sodium aluminate solubility. The increase in alumina solubility with ionic strength is due to the shift in the partition of hydroxide to aluminum tetrahydroxide ($\text{Al}(\text{OH})_4^-$) with increasing sodium concentration.

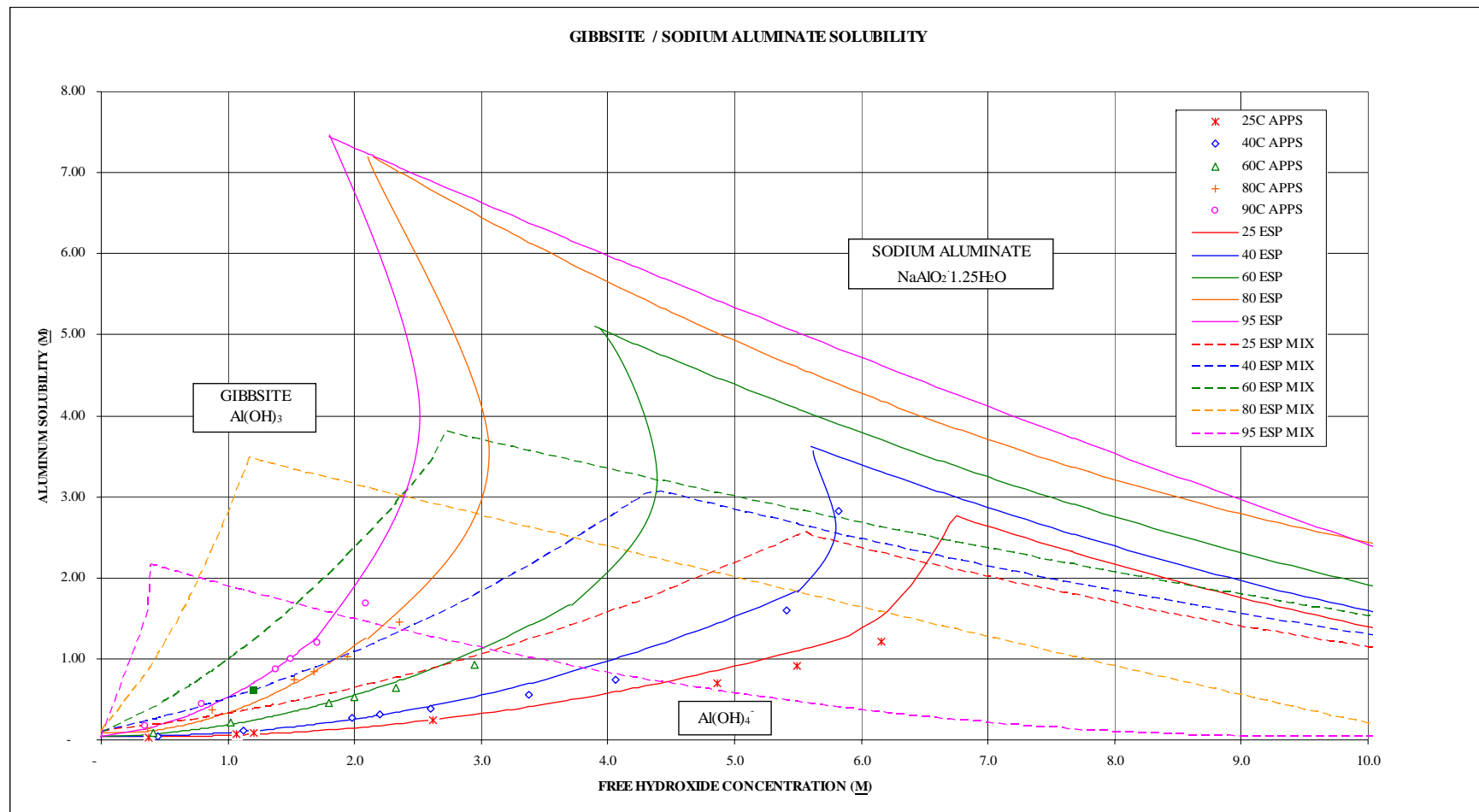


Fig. 3. Aluminum solubility versus free hydroxide diagram.

It is desirable to maintain alumina in solution during the crystallization of sodium salts. This is because the kinetics of gibbsite crystallization are far slower than sodium salt crystallization and supersaturation of gibbsite can result in amorphous, high-viscosity gel formation.

During crystallization of sodium salts, evaporation increases free hydroxide concentration and ionic strength of the solution. Thus, in most cases, alumina becomes more soluble up to the sodium aluminate phase boundary during the evaporative crystallization process.

CONCLUSION

Equilibrium modeling has limitations in modeling fractional crystallization. Firstly, although sodium salts rapidly achieve equilibrium in aqueous solution, metals (such as alumina) do not. Thus, although metal and mineral precipitates may be thermodynamically favored, their formation may be kinetically limited. Secondly, although the models can accurately predict solubility of salts in known solutions (i.e. simulants), the accuracy of the model is limited to the accuracy of the sampling and analysis of an unknown material (i.e. large non-homogeneous waste tanks). Thirdly, a thermodynamic model cannot predict solubility of unknown compounds. Finally, although the model can predict a theoretical Decontamination Factor (DF - ratio of influent activity to effluent activity), the actual DF achieved depends heavily on solid/liquid separation and washing efficiencies which can not be predicted by thermodynamic modeling alone.

Despite the limitations, thermodynamic modeling has proven very valuable in understanding multi-component solubility, planning crystallization experiments [6], and developing the fractional crystallization process. Thermodynamic modeling has accurately predicted salt saturation points, yields, and extent of decontamination in fractional crystallization laboratory studies. Results of this work can be reviewed in Reference 10 and Reference 11.

ACKNOWLEDGEMENTS

Funding for the thermodynamic modeling work was provided by the U.S. Department of Energy – Office of River Protection through its prime contractor, CH2M HILL Hanford Group, Inc. as part of the Hanford Medium/Low Curie Waste Pretreatment Project.

REFERENCES

1. WTPBASE databank was developed by OLI Systems for use on Hanford waste chemistry.
2. U.S. Patent 6,787,120, Volume Reduction of Aqueous Waste by Evaporative Crystallization of Burkeite and Sodium Salts, September 7, 2000, Geniesse, D.
3. Shi, B., Rousseau, R., "Structure of Burkeite and a New Crystalline Species Obtained from Solutions of Sodium Carbonate and Sodium Sulfate," J. Phys. Chem. B. 2003, 107, 6932-6937.

4. The backward curve of the gibbsite phase boundary is caused by the formation of sodium aluminate 2.5 hydrate. This precipitation removes water from solution, thus increasing the concentration (shown in weight percent) of aluminum in solution. If the diagram were on a molality scale, the “backward curve” would not exist.
5. NUREG/CR-5271, “Thermochemical Properties of Gibbsite, Bayerite, Boehmite, Diaspore, and the Aluminate Ion Between 0 and 350°C,” J. A. Apps, J. M. Neil, C. H. Jun, Lawrence Berkeley Laboratory, Earth Science Division, Cyclotron Road, Berkeley, CA 94720.
6. D. L. Herting, E. A. Nelson, R. W. Rousseau, *Fractional Crystallization of Hanford Single-Shell Wastes – Laboratory Development*, Waste Management 2007, Paper No. 7229.
7. U.S. Patent 6,787,120, volume Reduction of Aqueous Waste by Evaporative Crystallization of Burkeite and Sodium Salts, September 7, 2000, D. Geniesse.
8. B. Shi, R. Rousseau, *Structure of Burkeite and a New Crystalline Species Obtained from Solutions of Sodium Carbonate and Sodium Sulfate*, J. Phys. Chem. B. 2003, 107, 6932-6937.
9. NUREG/CR-5271, *Thermochemical properties of Gibbsite, Bayerite, Boehmite, Diaspore, and the Aluminate Ion Between 0 and 350 °C*, J.A. APPS, J.M. NEIL, C.H. JUN, Lawrence Berkeley Laboratory, Earth Science Division, Cyclotron Road, Berkeley, CA 94720.
10. R.W. Rousseau, H. Alsyouri, G. Dumont, and L. Nassif, “Hanford Medium/Low Curie Waste Pretreatment project - Phase I Laboratory Report,” RPP-RPT-27239 Rev. 0, January 2006.
11. *Fractional Crystallization Flowsheet Tests with Actual Tank Waste*, RPP-RPT-31352 Rev. 0 (prepared by D.L. Herting, CH2M HILL Hanford Group, Inc., October 2006 contract No. DE-AC27-99RL14047.